

Particle size analysis on density, surface morphology and specific capacitance of carbon electrode from rubber wood sawdust

E. Taer, B. Kurniasih, F. P. Sari, Zulkifli, R. Taslim, Sugianto, A. Purnama, Apriwandi, and Y. Susanti

Citation: [AIP Conference Proceedings](#) **1927**, 030006 (2018);

View online: <https://doi.org/10.1063/1.5021199>

View Table of Contents: <http://aip.scitation.org/toc/apc/1927/1>

Published by the [American Institute of Physics](#)

Particle Size Analysis on Density, Surface Morphology and Specific Capacitance of Carbon Electrode from Rubber Wood Sawdust

E. Taer^{1, a)}, B. Kurniasih^{1, b)}, F. P. Sari¹, Zulkifli¹, R. Taslim², Sugianto¹,
A. Purnama¹, Apriwandi¹ and Y. Susanti¹

¹*Department of Physics, University of Riau, 28293 Simpang Baru, Riau, Indonesia*

²*Department of Industrial Engineering, Islamic State University of Sultan Syarif Kasim, 28293 Simpang Baru, Riau, Indonesia*

^{a)}Corresponding author: erman_taer@yahoo.com

^{b)}bulqiskurniasih96@gmail.com

Abstract. The particle size analysis for supercapacitor carbon electrodes from rubber wood sawdust (SGKK) has been done successfully. The electrode particle size was reviewed against the properties such as density, degree of crystallinity, surface morphology and specific capacitance. The variations in particle size were made by different treatment on the grinding and sieving process. The sample particle size was distinguished as 53-100 μm for 20 h (SA), 38-53 μm for 20 h (SB) and $\leq 38 \mu\text{m}$ with variations of grinding time for 40 h (SC) and 80 h (SD) respectively. All of the samples were activated by 0.4 M KOH solution. Carbon electrodes were carbonized at temperature of 600°C in N_2 gas environment and then followed by CO_2 gas activation at a temperature of 900°C for 2 h. The densities for each variation in the particle size were 1.034 g cm^{-3} , 0.849 g cm^{-3} , 0.892 g cm^{-3} and 0.982 g cm^{-3} respectively. The morphological study identified the distance between the particles more closely at 38-53 μm (SB) particle size. The electrochemical properties of supercapacitor cells have been investigated using electrochemical methods such as impedance spectroscopy and charge-discharge at constant current using Solatron 1280 tools. Electrochemical properties testing results have shown SB samples with a particle size of 38-53 μm produce supercapacitor cells with optimum capacitive performance.

INTRODUCTION

Supercapacitor is an energy storage device other than capacitors, batteries and fuel cells [1]. In the last decade, supercapacitor has been widely used as an energy resource in electronic devices, electric cars and some other devices that require relatively faster energy transfer than batteries [2]. The supercapacitor component consists of two current collectors, two electrodes, a separator and an electrolyte located within the pores of the electrode [3]. Electrodes play an important role in determining energy and power that can be stored in supercapacitor cells. Usually, the electrode is selected from a conductor material with a high surface area such as activated carbon, which can be made from an organic material such as biomass materials. The selection of certain biomass materials as a precursor to produce active carbon electrodes has an advantage of self-adhesive characteristic after going through a compression process, another advantage is abundant availability, a friendly environment and stable in physical and chemical characteristics [4,5]. One of the factors that determine the strength of the electrode after compression process is the particle size of the material [6]. The optimum particle size will produce an electrode with optimum strength as well. The electrodes strength will be proportional to the density and electrical conductivity but inversely proportional to the porosity. Porosity properties, especially surface area are one of the key factors in producing supercapacitors with the higher energy. The balance of electrical conductivity and porosity properties influenced by particle size becomes the determining factor in producing supercapacitor electrodes from biomass material. In this paper the effect of particle size in the supercapacitor electrodes to the physical and electrochemical properties were discussed.

EXPERIMENT

The preparation of carbon electrodes is done by grinding process after the pre-carbonization stage. Carbon electrode are made by varies grinding time to find the difference in particle size. Raw materials (rubber wood sawdust) after ball milling process for 20 h and then sieved with 38 μm , 53 μm and 100 μm sieve sizes. The sieved sample with size 38 μm was continued with ball milling process for 40 h and 80 h to obtain a smaller particle size than 38 μm . Particle size of rubber wood sample can be divided into 4 groups i.e (i). 53-100 μm , (ii) 38-53 μm , (iii) ≤ 38 μm and (iv) is much smaller than the sample and labeled as SA, SB, SC and SD, respectively. All samples were activated using KOH with a concentration of 0.4 M [7]. The green electrode prepared using hydraulic press tool with a compression pressure of 8 tons. Furthermore, carbonization process was performed at a temperature of 600°C using nitrogen gas and continued with the physical activation process at a temperature of 900°C for 2 h using CO₂ gas [8] which aims to enlarge the pore diameter to increase surface area and electrical conductivity, resulting in the pellet carbon electrode. The produced sample was polished to obtain the electrode with thickness of 0.2 mm and then washed until neutral pH. Physical properties of the electrode measured were density and surface morphology. Electrochemical properties of the supercapacitor cell measured were specific capacitance, cell capacitance, energy density and power density based on the previous references [9 -10]. Measurement of electrochemical properties of supercapacitors were done by electrochemical impedance spectroscopy (EIS) and constant current charge discharge (CDC) using a 1286 solatron interface. Specific energy and power was calculated with the formula as given in equation (1) and (2) [11].

$$E = \frac{VIt}{m} \quad (1)$$

$$P = \frac{IV}{m} \quad (2)$$

RESULTS AND DISCUSSION

Figure 1 shows that the densities are 1.034 g cm⁻³, 0.849 g cm⁻³, 0.892 g cm⁻³ and 0.982 g cm⁻³ for SA, SB, SC and SD electrodes, respectively.

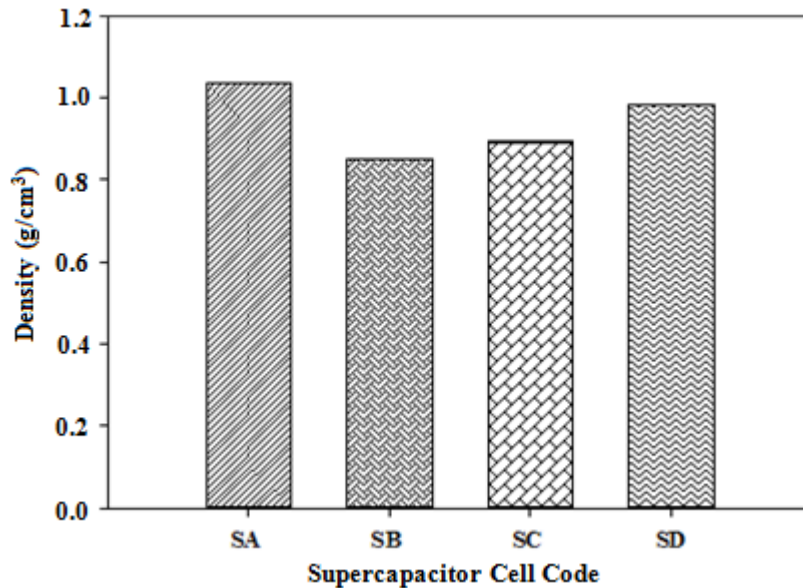


FIGURE 1. The density of carbon electrodes for various samples

The highest density is for SD electrode because of the longest grinding time and predicted the sample has the smallest particle size. While the smallest density is obtained for SA electrode because of its largest particle size, so this electrode has large number of macro pores that appear in between the particle boundary. The data shown in Fig. 1 does reveal any indication for such an explanation already mentioned. This condition can occur due to several factors, such as the release of gas and the reconstruction of particles after the process of chemical and physical activation. Short grinding time causes large particle with macropores, while the long grinding time

produces a small particle size that produces micropores between the particles. This factor plays an important role in the pores formation, more pores are formed the density will be smaller because the mass of electrode decreased during the activation process. The SC and SD electrodes run into a longer grinding process compared to SB. It is can be certain that particle size produced after grinding process is smaller than SB electrode. After chemical activation then particle size will be smaller because during the activation process, excessive pore formation causes the sample decompose or break. This sample will produce a denser electrode than SB after the process. This is a reason for the higher electrode density of SC and SD than SB electrode. Smaller the pore, lesser the pore distribution and greater the density.

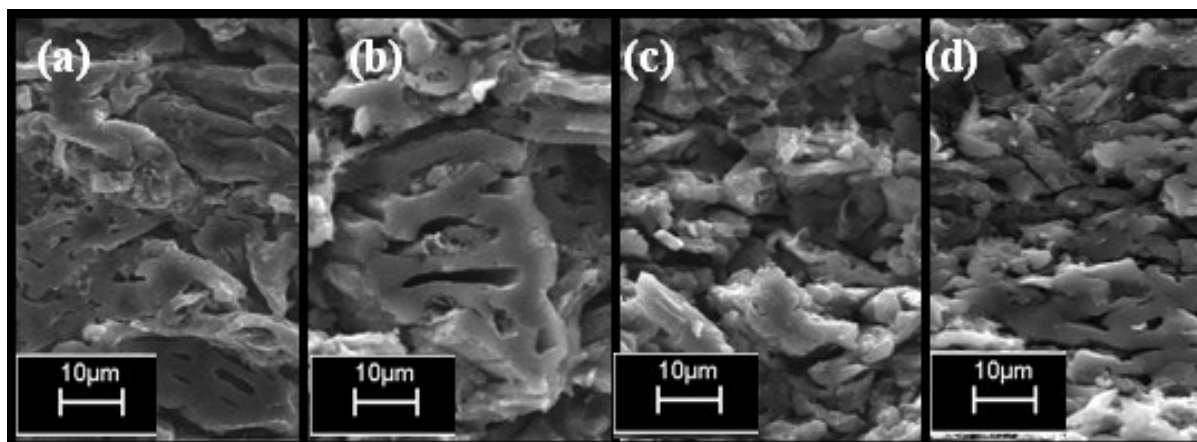


FIGURE 2. SEM micrograph of electrode cross sectional part with 500x magnification, (a) SA, (b) SB, (c) SC, (d) SD

Figure 2 shows the surface morphology on cross section part of the carbon electrode. In Fig. 2 the particles of the electrode have pores distributed uniformly. The carbon surface has more porous characteristics with the predominance of the macropores while meso and micropores were not see clearly. Figs. 2a and 2b show that SA and SB electrodes display a more open pore shape than the SC and SD electrodes shown in the Figs. 2c and 2d. The surface of SC and SD electrodes have a denser arrangement with slight pores. The pore distribution at the surface of SC and SD electrodes tend to be closed and smaller in size than the SA and SB electrodes.

Figure 3a shows the difference shape of Nyquist plot for each electrode. Generally, the Nyquist plot consists of only one semicircle [6], but in these two cells, there are actually two semicircular curves. The shortest curve line to the Z'' axis is exhibited by SB electrode which is then followed by SA, SC and SD electrodes. The C' vs. frequency curve can be seen in Fig. 3b shows different pattern for each of supercapacitor electrodes. Separation of C' for all samples occurs at a frequency of 2.04 Hz and a total separation occurs at a frequency of 0.31-0.01 Hz. This shows that at these frequencies, the electrolyte ions have started to occupy the pores of the electrodes perfectly. The C'' vs frequency curve can be seen in Fig. 3c. The C'' has significant changes at low frequency. The curve begins to split at a frequency of 25.13 Hz and totally separates at a frequency of 2.419-0.01 Hz. An increase in C'' occurs because the electrolyte ions can access pores of electrode well at the low frequency region. Maximum capacitance is generated when electrolyte ions have reached all the pore surfaces of the electrode [12]. The curve pattern in Fig. 3b has a different type with Fig. 3c i.e. the value of C'' decreased at a certain frequency for the four electrode samples which is caused the formation of the peak called as the peak frequency (f_p). This frequency describes the relaxation time of ions in the electrolyte when subjected to the charge-discharge [13] and the magnitude of C'' is directly proportional to the resulting C' .

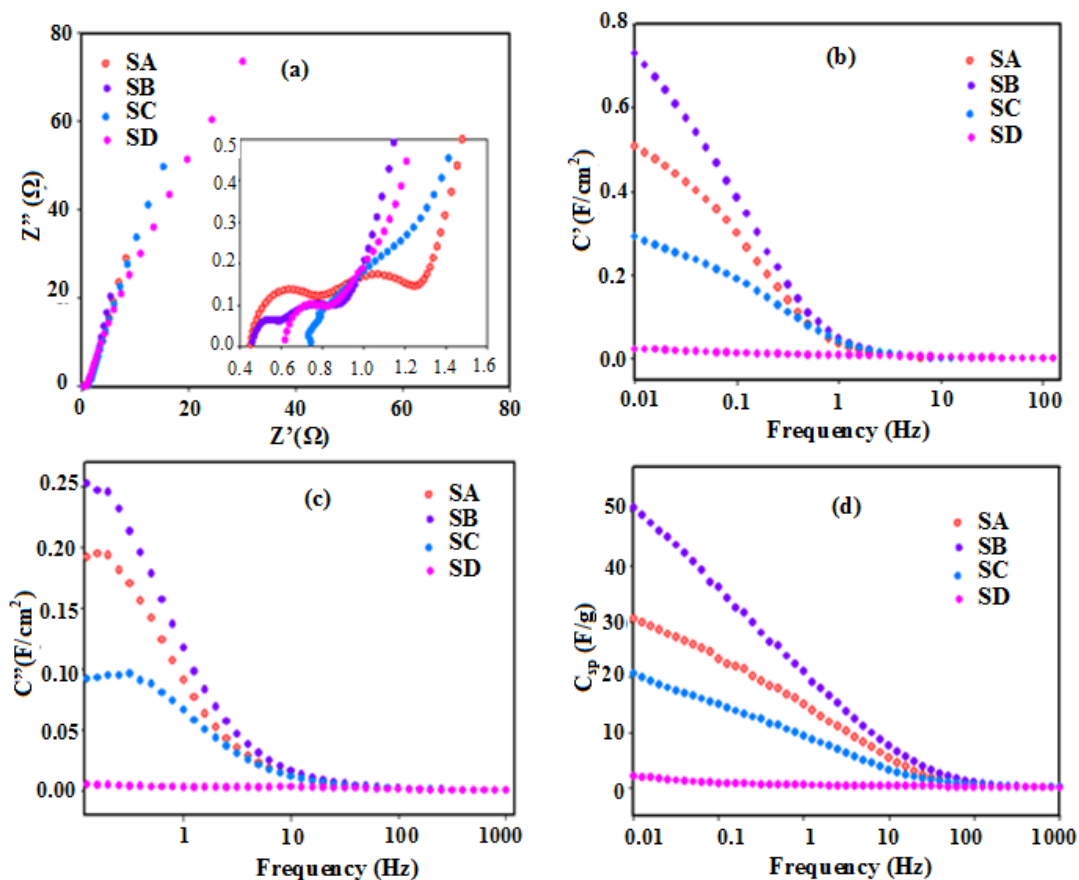


FIGURE 3. Nyquist plot for each sample, (a) riil impedance vs imajiner impedance (b) riil capacitance vs frequency (c) imaginary capacitance vs frequency (d) capacitance specific vs frequency

In Fig. 3d it can be noted that the specific capacitance (C^{sp}) shows a constant value at a frequency of 209.47 Hz - 1 kHz for all electrodes. The curve begins to split at a frequency region of 100.04 Hz and total separation occurs at a frequency of 16.86-0.01 Hz. Frequency affects the magnitude of specific capacitance, the greater is the frequency, smaller the capacitance, because specific capacitance is inversely proportional to frequency. The specific capacitance by EIS method for each sample of SA, SB, SC and SD were 30.52 F/g, 50.63 F/g, 20.67 F/g and 2.05 F/g, respectively. The specific capacitance using wood materials obtained was 234 F/g and 189 F/g for poplar wood [14] and fir wood [15]. Galvanostatic Charge-Discharge (GCD) measurement data was shown in Fig. 4. Patterns formed in the curve show that variations in particle size affect the discharge time for each cell, the curves show a significant difference for all cells. The data distribution in SD cells is very small, unlike the other three cells. It can be seen in the Fig. 4 that longer discharge time for SB cell and the shortest discharge time was for SD cells. Energy density and power density on supercapacitor are obtained by using GCD data at a constant current of 10 mA/s. The Ragone plot in Fig. 4b shows the different distribution of energy and power for all cells, when energy decreases the power increases and vice versa. The highest specific capacitance (C^{sp}) and cell capacitance (C^{cell}) of supercapacitor cells was obtained for SB supercapacitor cell, i.e., electrode with a particle size of 38-53 μm , while the lowest C^{sp} and C^{cell} were produced by SD cells with smallest particle size. This result corresponds to the picture obtained by the charge-discharge curve as shown in Fig. 4a. Cells with long discharge times will have a larger capacitance compared to cells with short discharge time.

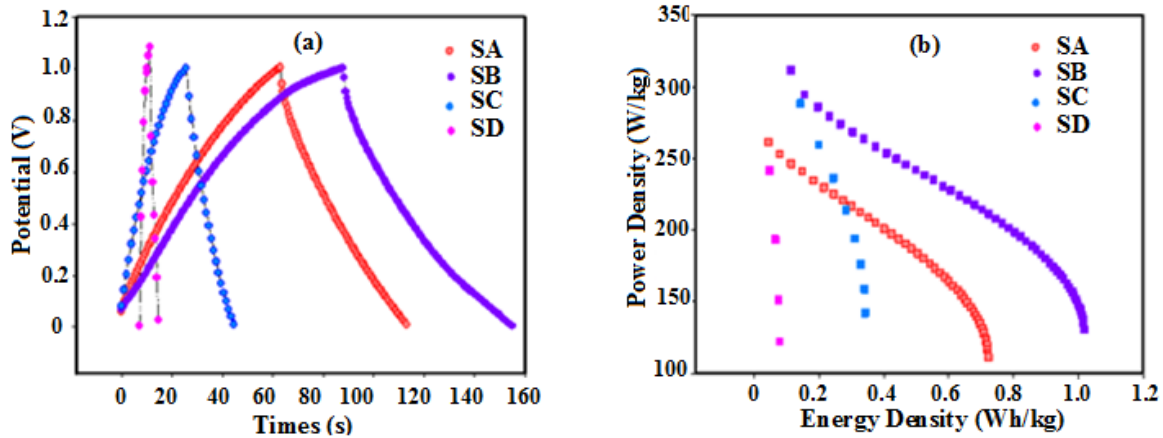


FIGURE 4. The charge-discharge curves for each sample (a) Energy density vs (b) power density

The GCD results were also coherent with the EIS results, as can be seen from Table 1. The SB cells has highest capacitive properties (Csp, Ccell, E, P).

TABLE 1. Energy Density, Power Density, Specific Capacitance and Cell Capacitance for various electrodes prepared

Sample Code	Particle Size	Mass (g)	E_{max} (Wh/kg)	P_{max} (W/kg)	Csp (F/g)		C (F)	
					GCD	EIS	GCD	EIS
SA	53-100	0.036	0.722	261.46	34.99	30.58	1.08	0.55
SB	38-53	0.031	1.017	311.58	43.01	50.65	1.54	0.78
SC	≤ 38	0.031	0.343	288.34	14.74	20.67	0.45	0.32
SD	$\leq SC$	0.035	0.079	241.70	2.14	2.05	0.07	0.03

CONCLUSION

Based on data and analysis, the particle size is an important factor that affects the physical properties such as density and surface morphology of the carbon electrodes. The physical properties of these electrodes clearly has effect on the electrochemical properties such as the specific capacitance, cell capacitance, energy and power density. The optimum particle size of the carbon electrode from rubber sawdust was achieved for 38-53 μm particle size with specific capacitance of 50.65 F/g, cell capacitance 0.785 F, energy and power as 1.01 Wh/kg and 311.58 W/kg, respectively.

ACKNOWLEDGEMENT

The authors acknowledge the DRPM for the research funding by HIBAH KOMPETENSI the third year (2017) with the project title "Nano Karbon Berbasis Biomassa sebagai Inti Elektroda Campuran untuk Superkapasitor".

REFERENCES

1. A. Burke, *Electrochim. Acta* **53**, 1083-1091 (2007).
2. P. Simon and A. Burke, *The Electrochem. Soc. Inter.* **17**, 38-43 (2008).
3. A. Burke, *J. Power Sources* **91**, 37-50 (2000).
4. R. Jihye, S. Y. Woong, S. D. Jin and A. D. June, *Carbon* **48**, 1990-1998 (2010).
5. N. Brun, S. Ken, Y. Linghui, G. Lars, M. Antonietti and M. M. Titirici, *Adv. Mater.* **22**, 1-16 (2012).
6. E. Taer, M. Deraman, I. A. Talib, Awitdrus, S. A. Hashmi and A. A. Umar, *Inter. J. Electrochem. Sci.* **6**, 3301-3315 (2011).
7. E. Taer, Iwantono, S. T. Mani, R. Taslim, D. Dahlan and M. Deraman, *Adv. Mater. Res.* **896**, 179-182 (2014).
8. E. Taer, M. Deraman, I. A. Talib, S. A. Hashmi and A. A. Umar, *Electrochim. Acta* **56**, 10217-10222 (2011).

9. L. Xi-Miao, Z. Rui, Z. Liang, L. Dong-hui, Q. Wen-ming, Y. Jun-he and L. Li-cheng, *New Carbon Mater.* **22**, 153-158 (2007).
10. H. Wang, H. Yi, X. Chen and X. Wang, *J. Mater. Chem.* **2**, 3223-3230 (2014).
11. E. Taer, R. Taslim, Z. Aini, S. D. Hartati and W. S. Mustika, "Activated carbon electrode from banana-peel waste for supercapacitor applications," in *The 6th International Conference On Theoretical And Applied Physics (The 6th Ictap)*, AIP Conference Proceedings 1801, edited by D. Tahir *et al.* (American Institute of Physics, Melville, NY, 2017), pp. 0400041-0400044.
12. C. Potret, P. L. Taberna, P. Simon and C. Laberty-Robert, *Electrochim. Acta* **49**, 905-912 (2004).
13. J. Segaini, B. Daffos, P. L. Taberna, Y. Gogotsi and P. Simon, *Electrochim. Acta* **55**, 7489 (2009).
14. M. C. Liu, B. Kong, P. Zhang, Y. C. Luo and L. Kong *Electrochim. Acta* **60**, 443-448 (2011).
15. B. Lu, L. Hu, H. Yin, W. Xiao and D. Wang. *RSC Adv.* **6**(108), 106485-106490 (2016).